Design, synthesis, and biological evaluations of novel oxindoles as HIV-1 non-nucleoside reverse transcriptase inhibitors. Part 2

11 AUTHORS, INCLUDING:

ELSEVIER

Design, synthesis, and biological evaluations of novel oxindoles as HIV-1 non-nucleoside reverse transcriptase inhibitors. Part 2

Tao Jiang, Kelli L. Kuhen, Karen Wolff, Hong Yin, Kimberly Bieza, Jeremy Caldwell,
Badry Bursulaya, Tove Tuntland, Kanyin Zhang,
Donald Karanewsky and Yun He*

Genomics Institute of the Novartis Research Foundation (GNF), 10715 John Jay Hopkins Drive, San Diego, CA 92121, USA

Abstract—A series of heterocycle-containing oxindoles was synthesized and their HIV antiviral activities were assessed. Some of these analogs exhibited potent inhibitory activities against both wild-type virus and a number of drug-resistant mutant viruses. In addition, oxindole **9z** also showed promising pharmacokinetics.
© 2006 Elsevier Ltd. All rights reserved.

Highly active antiretroviral therapy (HAART) is the standard of care for AIDS patients. The majority of HIV-infected individuals are currently taking reverse transcriptase inhibitors as a critical part of HAART. However, during the long-term therapy, resistance to chemotherapy can develop in a significant number of patients. In recent years, resistance and cross-resistance to all marketed reverse transcriptase inhibitors have become an increasing problem in the treatment of AIDS patients.[1–8] There is an urgent need to develop novel classes of reverse transcriptase inhibitors that are effective against the drug-resistant mutants.

In the previous report, we disclosed the discovery of a series of novel oxindoles as HIV-1 non-nucleoside reverse transcriptase inhibitors as well as their preliminary SAR.[9] Oxindole **1** is a potent inhibitor for HIV replication (Fig. 1). Unfortunately, it exhibited extremely high clearance, low exposure, and low oral bioavailability. Therefore, our next effort was directed to optimizing the physicochemical properties for this series of compounds. Oxindole **1** had poor rat liver microsomal stability in vitro, which was presumably the cause for its low exposure. Since ester moieties are known to be metabolically unstable, our first effort was to replace the ester moiety with its bioisosteric tetrazole.
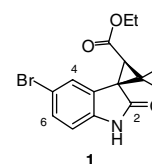
Figure 1.

The synthesis of the tetrazole analogs **6** and **7** is shown in Scheme 1. Wittig reaction of isatin **2** gave the corresponding olefin **3** in excellent yield. Olefin **3** was
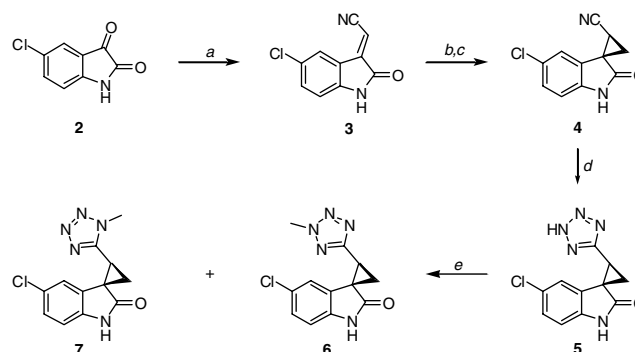
Scheme 1. Synthesis of tetrazole analogs **6** and **7**. Reagents and conditions: (a) CNCHPPh$_3$ (1.2 equiv), benzene, 80 °C, 4 h, 95%; (b) CH$_2$N$_2$ (excess), Et$_2$O, 0–25 °C, 5 h; (c) toluene, reflux, 8 h, 65% over 2 steps; (d) N$_3$SnMe$_3$ (1.5 equiv), xylene, reflux, 16 h, 89%; (e) CH$_2$N$_2$ (excess), Et$_2$O, 0 °C-25 °C, 1 h, 50% (**6**:**7** = 2:1).

then treated with diazomethane at room temperature followed by refluxing in xylene to provide the spiral oxindole **4** in moderate yield. Nitrile **4** reacted with azidotrimethyltin to afford tetrazole **5** in excellent yield. Methylation of **5** using diazomethane led to a 2:1 regioisomeric ratio of **6** and **7**. Their structures were established by NOSEY studies. Not surprisingly, tetrazole **5** was inactive against HIV virus, as it is the equivalent of the corresponding acid (Table 1). Tetrazole **6** showed strong inhibition against HIV virus with almost equal potency to its ester analog. On the other
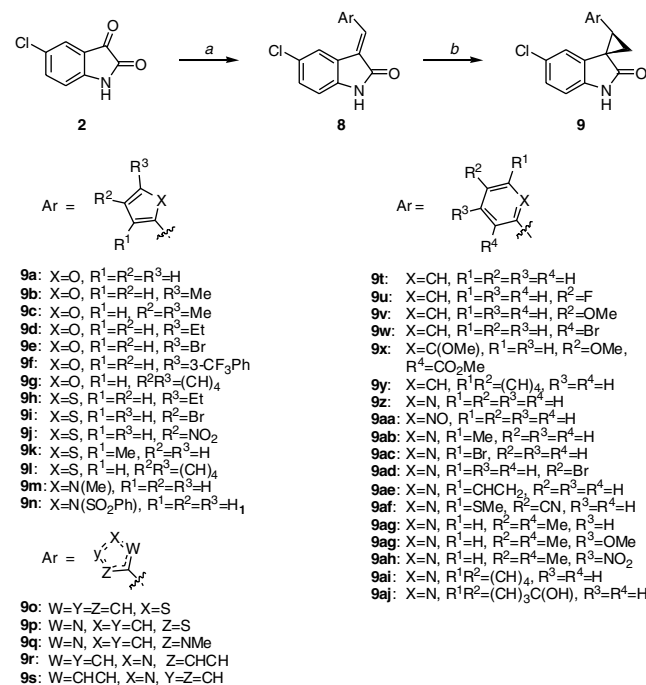
hand, compound **7** was inactive, as the methyl group was presumably placed at the wrong position in the binding pocket.

Encouraged by this result, we decided to further explore the ester region and seek for additional replacement for the ester/tetrazole moiety. A library of analogs with aryl or heteroaryl moieties in the place of the ester/tetrazole was rapidly synthesized in a two-step sequence for biological evaluations (Scheme 2). Reaction of isatin **2** with various aryl or heteroaryl aldehydes furnished the corresponding olefins **8a–8aj**. Under rhodium (II) acetate catalysis, olefin **8** reacts with diazomethane to afford various aryl and heteroaryl analogs **9a–9aj**. Interestingly, the simple furan analog **9a** exhibited a 200 nM EC_{50}, whereas the monomethyl and dimethyl analogs (**9b** and **9c**) showed an EC_{50} of 73 and 27 nM, respectively. These data suggest the critical role of the methyl groups in filling the corresponding hydrophobic pocket. Analogs with bulkier substitutions on the furan ring (**9d**, **9e**, and **9f**) had decreased inhibitory activities, suggesting that the pocket has limited space, while structurally rigid analog **9g** showed potent activity.

Among the 2-thiophene analogs (**9h–9l**), only the 5-ethyl analog (**9h**) exhibited strong inhibition. Replacement of the ethyl group with a polar nitro group at the 5 position (**9j**) completely abolished the inhibitory activity, as expected. The 2-methyl analog **9k** lost activity significantly, and this could be a result of the steric interaction between the methyl group and the oxindole ring, which forces one of the rings to adopt a conformation that results in unfavorable binding (Fig. 2). Interestingly, the 3-thiophene analog **9o** showed the highest activity,

Table 1. Anti-HIV activities of oxindoles[10,11]

Compound	EC_{50} (μM)	CC_{50} (μM)
Efavirenz	0.0005	~10
Nevirapine	0.05	>10
1	0.015	>10
5	>10	7.606
6	0.055	>10
7	>10	>10
9a	0.200	>10
9b	0.073	>10
9c	0.027	>10
9d	0.216	>10
9e	0.245	>10
9f	5.554	>10
9g	0.086	>10
9h	0.160	>10
9i	1.267	>10
9j	>10	>10
9k	0.844	>10
9l	4.967	>10
9m	>10	>10
9n	6.770	>10
9o	0.006	1.699
9p	>10	>10
9q	>10	>10
9r	>10	>10
9s	>10	>10
9t	0.244	>10
9u	>10	>10
9v	>10	>10
9w	>10	>10
9x	0.167	>10
9y	>10	>10
9z	0.008	>10
9aa	>10	>10
9ab	0.039	>10
9ac	0.023	>10
9ad	0.023	>10
9ae	0.005	>10
9af	0.436	>10
9ag	0.463	>10
9ah	0.18	>10
9ai	0.010	>10
9aj	0.587	>10
10a	0.018	7.949
10b	0.016	>10
10c	0.557	>10
10d	0.138	>10
10e	0.504	>10
10f	1.806	6.127
10g	0.648	>10
12a	0.028	5.238
12b	0.008	>10
12c	0.010	>10

9a: X=O, $R^1=R^2=R^3$=H
9b: X=O, $R^1=R^2$=H, R^3=Me
9c: X=O, R^1=H, $R^2=R^3$=Me
9d: X=O, $R^1=R^2$=H, R^3=Et
9e: X=O, $R^1=R^2$=H, R^3=Br
9f: X=O, $R^1=R^2$=H, R^3=3-CF$_3$Ph
9g: X=O, R^1=H, R^2R^3=(CH)$_4$
9h: X=S, $R^1=R^2$=H, R^3=Et
9i: X=S, $R^1=R^3$=H, R^2=Br
9j: X=S, $R^1=R^3$=H, R^2=NO$_2$
9k: X=S, R^1=Me, $R^2=R^3$=H
9l: X=S, R^1=H, R^2R^3=(CH)$_4$
9m: X=N(Me), $R^1=R^2=R^3$=H
9n: X=N(SO$_2$Ph), $R^1=R^2=R^3$=H

9t: X=CH, $R^1=R^2=R^3=R^4$=H
9u: X=CH, $R^1=R^2=R^3=R^4$=H, R^2=F
9v: X=CH, $R^1=R^3=R^4$=H, R^2=OMe
9w: X=CH, $R^1=R^2=R^3$=H, R^4=Br
9x: X=C(OMe), $R^1=R^3$=H, R^2=OMe, R^4=CO$_2$Me
9y: X=CH, R^1R^2=(CH)$_4$, $R^3=R^4$=H
9z: X=N, $R^1=R^2=R^3=R^4$=H
9aa: X=NO, $R^1=R^2=R^3=R^4$=H
9ab: X=N, R^1=Me, $R^2=R^3=R^4$=H
9ac: X=N, R^1=Br, $R^2=R^3=R^4$=H
9ad: X=N, $R^1=R^3=R^4$=H, R^2=Br
9ae: X=N, R^1=CHCH$_2$, $R^2=R^3=R^4$=H
9af: X=N, R^1=SMe, R^2=CN, $R^3=R^4$=H
9ag: X=N, R^1=H, $R^2=R^4$=Me, R^3=H
9ag: X=N, R^1=H, $R^2=R^4$=Me, R^3=OMe
9ah: X=N, R^1=H, $R^2=R^4$=Me, R^3=NO$_2$
9ai: X=N, R^1R^2=(CH)$_4$, $R^3=R^4$=H
9aj: X=N, R^1R^2=(CH)$_3$C(OH), $R^3=R^4$=H

9o: W=Y=Z=CH, X=S
9p: W=N, Y=Z=CH, Z=S
9q: W=N, Y=Z=CH, Z=NMe
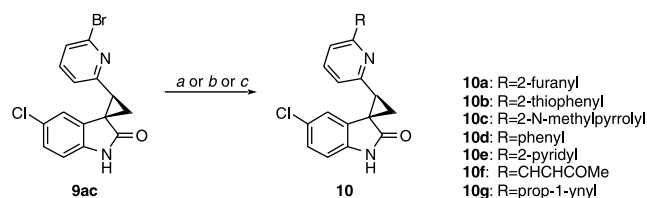**9r**: W=Y=CH, X=N, Z=CHCH
9s: W=CHCH, X=N, Y=Z=CH

Scheme 2. Synthesis of aryl analogs **9a–9aj**. Reagents and conditions: (a) ArCHO (1.5 equiv), piperidine (cat.), EtOH, 80 °C, 3–8 h, 65–80%; (b) CH$_2$N$_2$ (excess), Rh(OAc)$_2$ (cat.), CH$_2$Cl$_2$, 25 °C, 16 h, 40–65%.
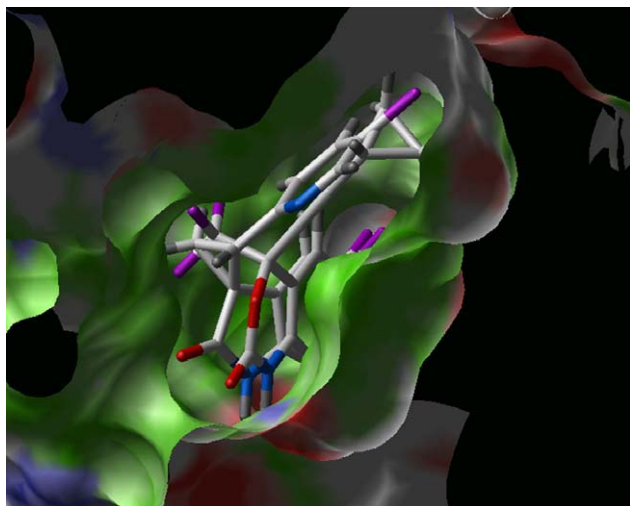
Figures 2. Docking of **9ad** and efavirenz into the HIV-1 NNRT site.[12]

presumably due to its optimum interaction with the enzyme in the hydrophobic pocket, although some cytotoxicity was observed in this analog. The pyrrole analogs (**9m**, **9n**), thiazole analog (**9p**), and imidazole analog (**9q**) are essentially inactive, which could be a result of the increased polar surface area and/or unfavorable steric interactions with the enzyme. A series of phenyl analogs (**9t**–**9y**) were also synthesized. Among these, only **9t** and **9x** showed moderate activity. While the 2-pyridinyl analog **9z** exhibited surprisingly single digit nanomolar EC_{50}, its isomers **9r** and **9s** were completely inactive, suggesting an important role of the pyridine nitrogen in the interaction with the enzyme.

Encouraged by the potent activity of **9z**, a series of 2-pyridyl analogs (**9aa**–**9aj**) were synthesized using the same chemistry (Scheme 2). Additional analogs **10a**–**10g** were prepared from **9ac** via Stille, Heck or Sonogashira couplings (Scheme 3). From the data in Table 2, it is very clear that small to medium size hydrophobic moieties as R^1 and/or R^2 are preferred for favorable interactions (Scheme 2), which was supported by molecular modeling studies (Fig. 2). Among these analogs, **9ac**, **9ad**, **9ae**, **10a**, and **10b** exhibited very potent inhibitory activity for HIV replication.

Molecular modeling studies were carried out to understand how these inhibitors interact with the HIV reverse transcriptase. The potent inhibitors in this series, such as **9ad**, could fit into the NNRTI binding pocket with high affinity (Fig. 2). Pyridyl analog **9ad** almost overlaps with efavirenz in space when docked into the NNRTI pocket. The cyclopropane moiety not only rigidifies the molecule for a proper fit into the pocket, but also fits into the same hydrophobic pocket as the trifluomethyl moiety in efavirenz. The pyridine moiety, on the other hand, fits into another hydrophobic pocket as the cyclopropane moiety in efavirenz does. The lactam NH in both molecules interacts with the K101 carbonyl oxygen via a critical hydrogen bond.

From previous SAR and molecular modeling studies,[9] we have learned that gem-dimethyl substitutions on the cyclopropane ring could potentially enhance the potency in the original ester series. To find out if the same enhancement could happen when the ester moiety is replaced with heterocycles, analogs **12a**–**12c** were synthesized in moderate yields by reacting **9ac**, **9ae**, and **9ai** with 2-diazopropane (**11**), respectively (Scheme 4). As expected, all three gem-dimethyl analogs showed potent anti-HIV activity.
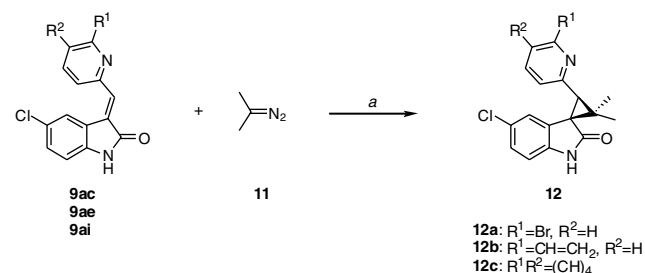
With wild-type potency established, we began to determine the mutant profile for this series. Selected oxindoles were screened against a panel of NNRTI-resistant mutants, and the data are shown in Table 3. Nevirapine (NVP) exhibits good antiviral activity against I135V and E138K mutant viruses, but is ineffective against viruses possessing the single mutations of K103N, V106A, Y181C or Y188L. NVP possesses only moderate activity in the submicromolar range against the remainder of the mutant viruses in the select panel. On the other hand, efavirenz (EFV) is effective against most of these mutant viruses, with the exception of Y188L. Most of the oxindoles showed decent antiviral

Table 2. Pharmacokinetics of **1** and **9z**[a]

Compound	$nAUC^b$ (min µg/mL)	nC_{max} [b] (nM)	$F\%$
1	0.90	17.9	27
9z	5.43	68.4	46

[a] Winsor rats.
[b] po, 50 mg/kg; AUC and C_{max} are normalized to 1 mg/kg.

10a: R=2-furanyl
10b: R=2-thiophenyl
10c: R=2-N-methylpyrrolyl
10d: R=phenyl
10e: R=2-pyridyl
10f: R=CHCHCOMe
10g: R=prop-1-ynyl

Scheme 3. Synthesis of oxindoles **10a**–**10g**. Reagents and conditions: (a) For **10a**–**10e**: RSn^nBu_3 (1.3 equiv), $Pd(PPh_3)_4$ (cat.), toluene, reflux, 16–24 h, 40–85%; (b) For **10f**: acrylic acid methyl ester (3.0 equiv), $Pd(OAc)_2$ (cat.), PPh_3 (1.0 equiv), $NaHCO_3$ (1.0 equiv), DMF, 80 °C, 36 h, 65%; (c) For **10g**: CH_3CCH (1.5 equiv), $PdCl_2(PPh_3)_2$ (cat.), CuI (cat.), iPr_2NH_2:DMF = 1:1, 25 °C, 16 h, 85%.

12a: R^1=Br, R^2=H
12b: R^1=CH=CH$_2$, R^2=H
12c: R^1, R^2=(CH)$_4$

Scheme 4. Synthesis of oxindoles **12a**–**12c**. Reagents and conditions: (a) **11** (excess), Et_2O, 45 °C, 2–4 h, 45–57%.

Table 3. Antiviral activities (EC$_{50}$, µM) of selected oxindoles against HIV-1-resistant mutants[10]

Compound	WT	L100I	K103N	V106A	I135T	I135V	E138K	V179E	Y181C	Y188L	F227C	F227L
Efavirenz	0.0005	0.010	0.032	0.004	0.001	0.001	0.002	0.006	0.0011	0.28	0.008	0.001
Nevirapine	0.050	0.164	5.053	8.458	0.207	0.079	0.031	0.116	>10	>10	0.733	0.148
9c	0.027	0.260	>10	0.630	0.236	0.059	0.052	2.465	3.070	>10	0.957	0.063
9o	0.006	0.008	0.100	0.513	0.048	0.017	0.030	0.324	0.031	1.252	0.142	0.002
9z	0.008	0.174	>10	0.259	0.127	0.026	0.045	0.898	3.227	>10	0.528	0.013
9ac	0.023	0.277	1.928	0.166	0.046	0.014	0.032	0.048	0.134	6.518	0.145	0.048
9ae	0.003	0.178	11.096	0.149	0.016	<0.003	0.020	0.088	0.085	22.638	0.578	0.088
10a	0.018	2.087	14.280	2.516	0.076	0.055	0.028	0.101	0.265	23.106	0.658	2.354
10b	0.016	0.100	2.240	0.147	0.068	0.263	0.038	0.060	0.063	1.969	0.313	0.365
12b	0.008	0.228	0.696	0.041	0.037	0.029	0.026	0.010	0.120	1.068	0.087	0.014
12c	0.010	0.058	2.346	0.102	0.055	0.047	0.071	0.483	0.717	>10	2.075	0.381

activity against L100I, I135T, I135V, E138K, V179E, and F227L mutant viruses. However, similar to nevirapine and efavirenz, these oxindole analogs exhibited poor antiviral activity against K103N and Y188L. In general, the oxindoles are not as potent as EFV toward these mutants but are superior to NVP. A few of them, such as **9o** and **12b** have significantly improved mutant profiles compared to nevirapine. Further optimization would be required to achieve potency in all of these NNRTI-resistant mutant viruses.

In vitro studies suggested that many of these heterocycle-containing analogs have improved water solubility and metabolic stability. Compound **9z** was also studied for its pharmacokinetic properties in vivo. Compared to ester **1**, the pyridine analog **9z** showed significantly improved exposure (Table 2).

In summary, following a lead from previous studies, a series of oxindoles with aromatic moieties in the place of metabolically unstable ester moiety was synthesized, and a number of these analogs exhibited potent antiviral activity toward wild-type virus as well as certain drug-resistant mutants. Among these, compound **9z** also exhibited promising pharmaceutical properties.

References and notes

1. St. Clair, M.; Martin, J. L.; Tudor-Williams, G.; Bach, M. C.; Vavro, C. L.; King, D. M.; Kellam, P.; Kemp, S. D.; Larder, B. A. *Science* **1991**, *253*, 1557.
2. Sebastian, J.; Faruki, H. *Med. Res. Rev.* **2004**, *24*, 115.
3. Gotte, M. *Exert Rev. Anti-Infect. Ther.* **2004**, *2*, 707.
4. Mugavero, M. J.; Hicks, C. B. *Drug Discovery Today: Ther. Strategies* **2004**, *1*, 529.
5. Rusconi, S.; La Seta Catamancio, S.; Citterio, P.; Bulgheroni, E.; Kurtagic, S.; Galazzi, M.; Croce, F.; Moroni, M.; Galli, M. *Antiviral Ther.* **2001**, *6*, 41.
6. Miller, V.; Ait-Khaled, M.; Stone, C.; Griffin, P.; Mesogiti, D.; Cutrell, A.; Harrigan, R.; Staszewski, S.; Katlama, C.; Pearce, G.; Tisdale, M. *AIDS* **2000**, *14*, 163.
7. Pauwels, R. *Curr. Opin. Pharmacol.* **2004**, *4*, 437.
8. Bacheler, L. T. *Drug Res. Updates* **1999**, *2*, 56.
9. Jiang, T.; Kuhen, K. L.; Wolff, K.; Yin, H.; Bieza, K.; Caldwell, J.; Bursulaya, B.; Wu, T. Y.-H.; He, Y. *Bioorg. Med. Chem. Lett.* **2006**, *16*, 0000.
10. Antiviral efficacy assay: Compounds were serially diluted in DMSO and added to adherent HEK293T target cells prior to addition of VSV-g pseudotyped HIV-1 luciferase reporter virus (HIV-1 pseudovirions) harvested from 293T producer cells following a triple transient transfection (CaP, Clontech) of the three plasmid HIV-1 lentiviral vector system comprised of the VSV-g envelope expression plasmid, packaging construct (delta psi), and the HIV-1 LTR:Luc plasmid. The VSV-g envelope expression plasmid generates the pseudovirus receptor that permits a broad tropism and mediates entry into the 293T target cells. The delta psi packaging construct supplies all of the structural and regulatory gene products needed to generate the pseudovirus. The viral vector RNA synthesized from the HIV-1 LTR:Luc plasmid possesses the *cis* RNA packaging signal (psi sequence) in addition to the luciferase reporter gene and the HIV-1 LTR. The supernatants of transfected producer cells contain HIV-1 pseudovirions carrying only the luciferase gene in the viral genome. Upon transduction of the target 293T cells, the viral genomic RNA will undergo reverse transcription, nuclear translocation, integration, and transcription of the integrated luciferase gene driven by the PGK (phosphoglycerate kinase promoter). Luciferase activity using Bright-Glo reagent (Promega) substrate was measured 48 h post-infection using a CLIPR plate reader (Molecular Devices) to determine EC$_{50}$ values.
11. All compounds reported are racemic, and only one enantiomer is shown. Data are based on the measurement of the racemic mixture.
12. Flexible docking was conducted using Glide 2.0 (Schrodinger, Inc., Portland, OR, 2002). The protein coordinates were taken from protein databank (pdb code 1FK9).